Aerosol Science and Technology

ISSN: 0278-6826 (Print) 1521-7388 (Online) Journal homepage: https://www.tandfonline.com/loi/uast20

Coincidence in Time-of-Flight Aerosol Spectrometers: Phantom Particle Creation

William A. Heitbrink , Paul A. Baron & Klaus Willeke

To cite this article: William A. Heitbrink , Paul A. Baron & Klaus Willeke (1991) Coincidence in Time-of-Flight Aerosol Spectrometers: Phantom Particle Creation, Aerosol Science and Technology, 14:1, 112-126, DOI: 10.1080/02786829108959476

To link to this article: https://doi.org/10.1080/02786829108959476

Coincidence in Time-of-Flight Aerosol Spectrometers: Phantom Particle Creation

William A. Heitbrink and Paul A. Baron
Division of Physical Sciences and Engineering, National Institute for Occupational Safety and Health, Centers for Disease Control, 4676 Columbia Parkway, Cincinnati, Ohio 45226

Klaus Willeke
Aerosol Research Laboratory, Department of Environmental Health, University of Cincinnati, Cincinnati, Ohio 45267-0056

When using time-of-flight aerosol spectrometers, particle size measurement is based upon a particle's transit time between two laser beams. The particle's transit time is assumed to be the time difference between the two pulses of light that are produced as the particle passes through the two laser beams. Particle coincidence, which occurs when a second particle crosses the first laser beam before the first particle crosses the second laser beam, has a complex effect upon the measured size distribution. As a result of coincidence, time-of-flight aerosol spectrometers can replace real particles of one size with spurious, or phantom, particles of a different size in the measured distribution. When partial detection of a particle occurs, i.e., only one pulse from a particle is detected, another particle producing a pulse that occurs while the timer is open can cause the recording of a randomly sized phantom particle. The creation of these phantom particles, which we termed "open-timer" phantom particles, has been investigated theoretically and experimentally in a commercially available time-of-flight aerosol spectrometer. The number of these open-timer phantom particles was found to increase with particle size and aerosol concentration. In addition, the instrument's detection logic affects the number and size of the phantom particles. These are most apparent in the tails and minima of the measured distribution. In order to minimize phantom particle creation, the concentration of partially detected particles must be minimized. Strategies to reduce phantom particle concentration involve reducing the concentration of small particles near the optical detection threshold of the spectrometer.

INTRODUCTION

Time-of-flight aerosol spectrometers are used to make real-time measurements of an aerodynamic particle size distribution. An example of such an instrument is the aerodynamic particle sizer (APS, model 3310, TSI, Inc., St. Paul, Minn.), which measures aerodynamic diameter over the range of 0.5–32 μm. Because the nature of the hazard from the inhalation of an aerosol varies with aerodynamic particle size, such instruments are very useful in conducting health-related aerosol research. Baron (1986) noted that excess background counts were created by the APS. While using the APS to study filter penetration, Wake (1989) concluded that the APS can generate phantom or spurious particles. This study's purpose is to present and experimentally evaluate a theory that explains a mechanism for phantom particle generation by time-of-flight (TOF) aerosol spectrometers.

In order to understand phantom particle creation, one must understand the measurement techniques used in a TOF aerosol spectrometer. This instrument reports particle size as a function of aerodynamic diameter. The aerodynamic diameter of a particle is the diameter of a unit density sphere which has the same settling velocity in still air as the particle in question. TOF aerosol spec-

0278-6826/91/$0.00

Aerosol Science and Technology 14:112–126 (1991)
Published 1991 Elsevier Science Publishing Co., Inc.

trometers do not directly measure settling velocity. Instead, they are based on the principle that the magnitude of a particle's lag in an accelerating air flow is directly related to the particle's aerodynamic diameter. This lag is measured as the particle's transit time between two laser beams perpendicular to the flow. A timer measures the time difference or transit time between the light pulses produced by a particle passing through the two beams. The transit time is related to aerodynamic diameter through calibration with spheres of known density (e.g., polystyrene latex).

Figure 1 illustrates how a TOF aerosol spectrometer can interpret pulses to create phantom particles. The first particle's pulses are A_1 and A_2, and the second particle's pulses are B_1 and B_2. In case 1, the second pulse, A_2, of the first particle is too small to be detected. The electronic timer waits for a time (T) which defines the largest particle that is sized. A second particle arrives before the timer is turned off and the first pulse, B_1, of that particle is detected. The time between pulses A_1 and B_1 is recorded as a transit time. As a result, two real particles are deleted and one phantom particle is added to the measured size distribution. We define the latter as an open-timer phantom particle. Pulse B_2 starts the timer again, but it is ignored unless another pulse is detected before time T elapses. Case 2, which shows how instrument dead-time affects the creation of open-timer phantom particles, will be discussed later.

In order to create open-timer phantom particles, a TOF aerosol spectrometer must detect only one of a particle's two pulses. These single pulses can occur for a number of reasons. In many naturally occurring size distributions, number concentration increases dramatically with decreasing size. If there are many small particles present which create pulses at the detection limit for the signal processing within the TOF aerosol spectrometer, a large fraction of these particles will generate single pulses. Pulses within a pulse pair do not necessarily have the same amplitude, because of electronic noise or differences in the scattering efficiency between the two beams. For example, the parallel laser beams of the APS are polarized in different directions and may have slightly different intensities. As a result, the amount of light scattered by nonspherical particles may depend on the light's polarization.

In addition to partially detected particles, there are other sources of single pulses. If a particle's transit time is too long, the timer will be automatically turned off before the second pulse is detected. Thus, pulses from a very large particle may cause the timer to be turned on twice. If another pulse occurs between these two pulses, a phantom particle will be registered. Finally, the presence of a large number of very small particles, not normally producing pulses above the detection threshold, can increase the noise level in the detector, causing spurious peak detection. In all of these scenarios, the creation of phantom particles requires the presence of more than one particle and is, therefore, a coincidence phenomenon.

In case 3 of Figure 1, pulse B_1 of the second particle arrives before pulse A_2 of the first particle. As a result, the times between pulses A_1 and B_1 and between pulses A_2 and B_2 are measured as particle transit times. The net result is that the two real particles are replaced in the measured distribution by two smaller phantom particles. These phantom particles will be referred to as overlap phantom particles.

The occurrence rate of overlap phantom particles can be evaluated by using an equation (Jaenicke, 1972; Willeke and Liu, 1976) which describes the reduction in apparent concentration caused by coincidence in optical particle counters:

$$C_i = C_a \exp(-C_a Q t), \qquad (1)$$

where C_i = indicated concentration; C_a = actual concentration; Q = volumetric sample

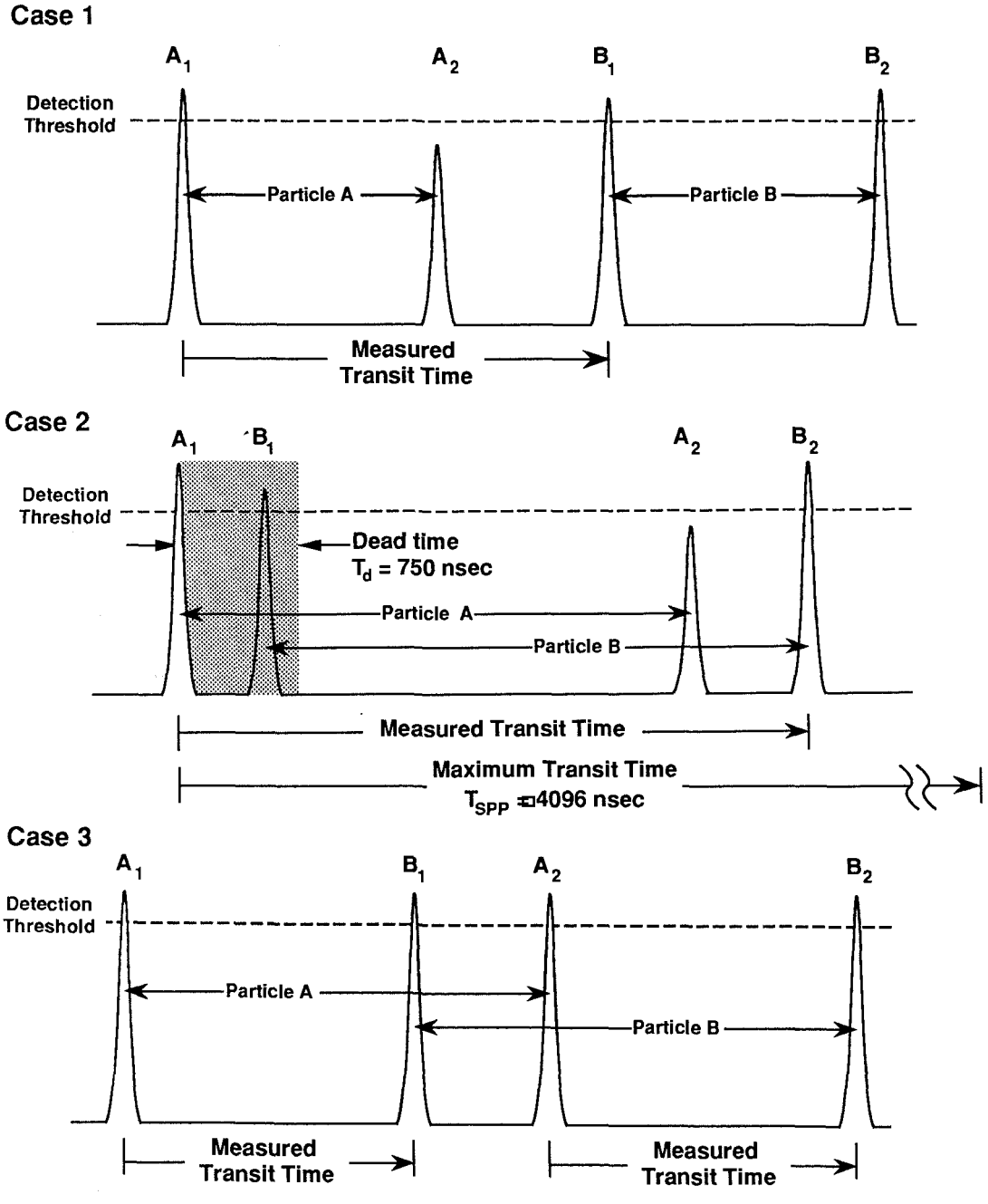

FIGURE 1. A schematic of the analog output of the aerodynamic particle sizer (APS) small particle processor. This illustrates the occurrence of coincidence in particle size measurements by the time-of-flight (TOF) detector. The measured transit times are based on the processor's particle counting rules. Case 1 represents open-timer phantom particle formation. Case 2 represents open-timer phantom particle formation caused by detector dead-time. Case 3 represents overlap phantom particle formation.

flow rate; and t = transit time through view volume in optical particle counter.

In order to apply this equation to TOF aerosol spectrometers, the particle transit time is used as the value of t in Eq. 1. This equation can be used to estimate the number of overlap phantom particles. The exact effect of overlap coincidence on the measured distribution will vary with the aerosol size distribution and the detection logic of the TOF aerosol spectrometer. Further analysis of overlap coincidence will not be presented in this paper.

Open-timer phantom particle creation was studied because it can bias measurements made with a TOF aerosol spectrometer at low measured concentrations. An analysis was performed to put the concepts discussed above on a mathematical basis for an idealized case to determine the rate of occurrence of open-timer phantom particles. This mathematical analysis was extended to the APS, taking into account its detection logic, which is designed to prevent phantom particle creation. Computer simulations also were conducted to fully consider the detection logic of the APS and to obtain the shape of the distribution of open-timer phantom particles. Experimental measurements were conducted with a polydisperse aluminum oxide aerosol to evaluate the theoretical analysis.

THEORY

The creation of open-timer phantom particles by a (simple) TOF aerosol spectrometer was investigated by analyzing the case of an aerosol containing two monodisperse particle modes. This theoretical analysis was then extended to the APS model 3310, including a consideration of its anticoincidence detection logic. The concepts developed in the analysis were generalized to a polydisperse aerosol using a Monte Carlo simulation.

Mathematical Analysis

Consider a bimodal aerosol distribution, with each mode being monodisperse. The larger particles have a concentration of C_f and are fully detected by the TOF aerosol spectrometer. The smaller particles have a concentration of C_s and are partially detected, because their pulse amplitudes are close to the detection threshold of the spectrometer.

When this bimodal aerosol is sampled by a TOF aerosol spectrometer, the individual pulses from the small particles are detected with efficiency p. This TOF aerosol spectrometer measures particle transit times with no logic to prevent phantom particle generation. The event tree in Figure 2 depicts the consequences of incomplete detection of the pulses from the small particles. When only one of a particle's two pulses is detected, the timer stays turned on. The event tree contains two paths in which this occurs and the concentration of these single pulses (C_{sp}) is:

$$C_{sp} = 2p(1-p)C_s. \tag{2}$$

The concentration of fully detected small particles (C_d) is:

$$C_d = p^2 C_s. \tag{3}$$

The estimated concentration of open-timer phantom particles created by the spectrometer is the product of the single pulse concentration and the probability of detecting a second pulse. The second pulses can occur because of fully or partially detected particles. At low concentrations when coincidence involves only two particles, this prob-

FIGURE 2. Event tree for the detection of a small particle near the detection threshold of a TOF aerosol spectrometer. p = Probability of pulse detection.

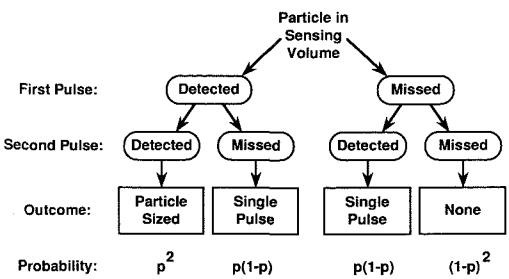

ability is the expected number (E_1) of single pulses and fully detected particle pulse pairs that occur in the volume sampled during time (T). T is the maximum transit time for the TOF aerosol spectrometer. If a second pulse is not detected by T, the timer is reset. The sampled volume is the product of T and the volumetric sampling rate (Q) of the instrument. The expected number of counts per single pulse (E_1) which can close the timer before the timer resets:

$$E_1 = (C_d + C_f + C_{sp})QT. \quad (4)$$

The concentration of open-timer phantom particles ($C_{ot,s}$) recorded by the TOF aerosol spectrometer is:

$$C_{ot,s} = C_{sp}E_1. \quad (5)$$

When E_1 is less than 0.1, more than 95% of the open-timer phantom particle creation occurs because of coincidence between a single pulse and either a completely detected particle or another single pulse. Because the arrival time of the second pulse is a random event, the single-pulse concentration will approximately follow a random uniform distribution with respect to transit time. At higher concentrations, multiple coincidence will occur and the distribution will be skewed to smaller particles.

Application to Aerodynamic Particle Sizer Model 3310

In order to apply Eq. 5 to the APS, the instrument's detection logic needs to be considered. The APS uses a single photomultiplier tube to detect the two pulses of light scattered by the particle as it passes through the two laser beams. Two signal processors, the small-particle processor (SPP) and the large-particle processor (LPP), independently use the time difference between the detector pulses to measure a particle's transit time and, hence, particle size. The SPP and LPP provide particle size information over two overlapping size ranges, resulting in a manufacturer-specified detection range of 0.5–32.8 μm. Particle sizes smaller than 5.23 μm are obtained just from the SPP aerodynamic size channels, and particles larger than 17.1 μm are obtained just from the LPP aerodynamic size channels. As particle size increases from 5.23 to 15.39 μm, the SPP size data is phased out and the LPP data is phased in.

In order to measure aerodynamic diameter, the SPP measures each particle's transit times digitally in increments of 4 ns from 750 to 4096 ns and stores the counts in accumulator channels 128–1024. The particle counting rules for the SPP are:

1. When a pulse larger than 0.02 V is detected, the timer is started.
2. If the first pulse is larger than 0.75 V, the threshold for the second pulse is increased from 0.02 to 0.75 V.
3. After the first pulse has been detected, all following pulses are masked for a 750-ns dead-time period (the transit time for air).
4. If a second pulse is detected before 4,096 ns have elapsed, a particle is counted and sized and the timer is reset to zero.
5. If 4,096-ns elapse after the first pulse and no other pulses have been detected, the timer is reset to zero.
6. While the timer is being reset, no pulses can be sensed for a period of 200 ns.

Cases 1 and 2 in Figure 1 describe the sequence of events which can cause the SPP to register open-timer phantom particles. In case 1, as discussed earlier, an open-timer phantom particle can be created when a single pulse is followed by either another single pulse or a fully detectable particle. When these second pulses arrive between 750 and 4096 ns after the first single pulse has started the timer, an open-timer phantom particle is counted. The expected number of these occurrences is given by Eq. 4, using the value of $Q = 16.6$ cm^3/s and $T = 4096 - 750$, or 3346 ns and the concentration of

open-timer phantom particles can be computed by Eq. 5.

Case 2 in Figure 1 shows how instrumental dead-time can result in the generation of open-timer phantom particles. A second particle arrives at the first laser beam during the dead-time period (T_d = 750 ns). Pulse A_2 is below the detection threshold. If particle B's transit time is less than 4096 ns $- t_2$, where t_2 is the arrival time of the second pulse after the initiating pulse, pulse B_2 will close the timer and an open-timer phantom particle will be added to the distribution. As a result, a real particle is replaced by a larger phantom particle whose transit time is as much as 750 ns too long. Because the maximum particle size which can close the timer varies with t_2, only some of the fully detected particles which arrive during T_d close the timer as compared to all of the fully and partially detected particles for case 1. In addition, case 2 open-timer phantom particles have a 750-ns time interval for the arrival of the second pulses versus a 3346-ns time interval for case 1. Because case 1 is the predominate mechanism for creating open-timer phantom particles, formulas for estimating the concentration and distribution of case 2 open-timer phantom particles are not presented in this paper.

In order to measure aerodynamic diameter, the LPP measures particle transit times in 66.67 ns increments and the counts are stored in accumulator channels 0–127. The counting rules for the LPP are:

1. Each pulse in the pulse pair must have an amplitude greater than 3 V.
2. No pulse greater than an interference threshold of 0.5 V may occur less than 8400 ns before the first pulse of the pulse pair, within 8400 ns of the trailing edge of the second pulse, or between the two pulses.
3. The maximum transit time is 8400 ns.
4. When the timer is being reset, all incoming pulses are ignored for an 840-ns period. The timer is reset when extraneous pulses are detected, when the time exceeds maximum transit time, and when a particle is registered by the LPP.

In order for the LPP to count a particle, its pulses must be completely isolated from other potentially interfering pulses. If a second particle with a pulse amplitude greater than 0.5 V arrives within 8400 ns of the first particle, both particles will be rejected by the LPP. This logic results in the rejection of all particles whose pulse pairs overlap, as well as some particles whose pulse pairs do not overlap and might have been properly sized. The creation of open-timer phantom particles by the LPP requires an extremely unlikely pulse pattern from two particles. Exactly one pulse from each particle must be above the 3-V threshold and the other pulse must be below the 0.5-V threshold. Furthermore, the two pulses which are greater than 3 V must be within 8400 ns of each other.

The SPP allows both overlap and open-timer coincidence to occur. On the other hand, the LPP virtually eliminates phantom particles. In order to study just the open-timer phantom particle creation, the detection system of the LPP was modified. After discussion with the APS manufacturer, a switch was installed to allow the detection threshold voltage for the LPP (rule 1 above) to be set at either 0.5 V or the normal 3.0 V. The analysis below uses the 0.5-V setting, referring to that processor version as the modified large particle processor (mLPP).

The mLPP can create open-timer phantom particles when two particles, each producing just one pulse exceeding the 0.5-V threshold, are within 8400 ns of each other. Because the second counting rule for the LPP is still in effect, the mLPP will reject particles which are affected by overlap coincidence. As a result, the expected number of acceptable second pulses for each single pulse (E_3) is:

$$E_3 = C_{sp} Q T_{LPP}, \quad (6)$$

where T_{LPP} is the maximum transit time (8400 ns) allowed by the LPP.

The estimated open-timer phantom particle concentration created by the mLPP is:

$$C_{ot,mLPP} = C_{sp}^2 Q T_{LPP}. \quad (7)$$

In the following sections, the combined data from the SPP and the mLPP are used to estimate the probability of pulse detection and the phantom particle concentration created by the mLPP.

Monte Carlo Simulation

The creation of phantom particles by the SPP and the mLPP was simulated by using Monte Carlo techniques. This simulation was performed to determine the open-timer phantom particle distribution with respect to transit time. This simulation implemented the logic associated with each processor and allowed coincidence to involve any number and size distribution of particles.

A Turbo Basic (Borland International, Scotts Valley, Calif.) program was written to create a stream of nearly one million particles, which were randomly spaced in a time period chosen to give the desired concentration. Particles were assigned diameters based upon the desired input size distribution. A mean pulse amplitude was assigned based on the measured response of our APS. The pulse width was assumed to be negligible, since the width was 10% or less of the typical time between pulses. The pulse amplitude for each particle was the sum of the mean pulse amplitude and a noise term. The noise term was the product of the pulse amplitude, the coefficient of variation, and a random normal deviate which was normally distributed with a mean value of 0 and a standard deviation of 1. The coefficient of variation was chosen to be 20% to reflect observed values. After sorting the individual pulses by arrival time, the pulse stream was analyzed according to the logic of the SPP and mLPP to produce a "measured" particle size distribution. Then, the particles were classified as either real particles, open-timer phantom particles (cases 1 and 2, Figure 1), or overlap phantom particles (case 3, Figure 1).

This Monte Carlo simulation used 20 million random numbers to create a stream of nearly one million particles. The random numbers were used as part of the procedure to determine each particle's arrival time, size, and pulse amplitude. Since the accuracy of a Monte Carlo simulation depends on the randomness of the computer's random number generator, the first 20 million random numbers produced by the computer were evaluated by using a chi-squared goodness-of-fit test (Whitney, 1984; Miller and Freund, 1977). The value of chi-squared was in the acceptance region at the 90% level of confience, indicating that the random number generator is sufficiently random for this application.

The following conditions were chosen, so that the SPP and mLPP generated open-timer phantom particles. The program was run with an input concentration of 400 particles/cm^3, a count median diameter of 0.5 μm and a geometric standard deviation of 1.15. This size distribution was chosen to straddle the detection threshold of the processor. Two runs of nearly one million particles were made, so that the SPP and the mLPP each had a pulse detection probability (p) of about 0.5. This resulted in a detected concentration of 100 particles/cm^3, the maximum value recommended by the APS manufacturer (TSI, 1987).

In Figure 3A and B, the number of open-timer phantom counts increases with aerodynamic diameter for the SPP and mLPP, respectively. Figure 3A and B also presents the number of phantom particles divided by aerodynamic channel width in nsec. These normalized counts increase slightly for the smaller phantom particles produced by the SPP, because of particles arriving during detector dead-time. Figure 3 indicates that the open-timer phantom particles created by the simulation of the mLPP logic closely

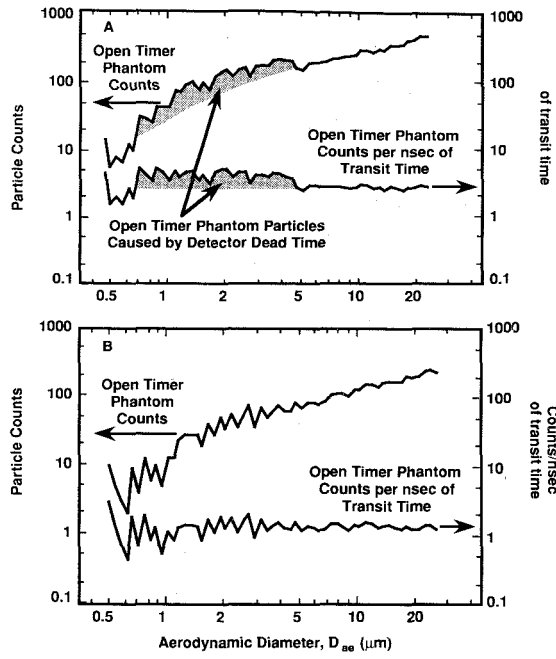

FIGURE 3. Size dependence of open-timer phantom particle counts generated by a Monte Carlo simulation of (*A*) the small particle processor (SPP) and (*B*) the modified large particle processor (mLPP) logic. The aerosol for these simulations had a count median diameter of 0.5 μm, a geometric standard deviation of 1.15, and a concentration of 400 particles/cm^3. For the SPP, a pulse amplitude of 0.02 V at 0.5 μm was used. For the mLPP, a pulse amplitude of 0.44 V at 0.5 μm was used. The upper curve in each figure is the result expected in the aerodynamic size distribution, while the lower curve indicates that the distribution of phantom counts is nearly uniformly distributed with respect to transit time.

follows a uniform distribution with respct to transit time. However, a Kolmogorov-Smirnov (KS) goodness-of-fit test (Gibson, 1971) indicates that there were slight, but significant, deviations between the observed distribution and a uniform distribution at the 99% confidence level. The KS test evaluates the maximum difference between the observed and expected cumulative difference function. For the mLPP data and the SPP data, the maximum observed deviations from a uniform distribution are, respectively, 0.019 and 0.08. A difference larger than 0.016 is significant at the 99% level of confidence. For the mLPP data, the observed deviation from a uniform distribution is too small to be noticeable or of any practical significance.

For the SPP data in Figure 3A, the number of phantom particles per nanosecond of transit time increases as particle size decreases below about 4 μm. The shaded area in Figure 3A is due to the arrival of fully detectable particles arriving during the 750-ns dead-time period (case 2, Figure 1). Because the transit time of a 0.5 μm particle is 800 ns, the second pulses from these particles can arrive as late as 800 ns after the dead-time period, resulting in a recorded transit time of 1,550 ns. This maximum, apparent transit time corresponds to an aerodynamic diameter of 4.5 μm.

When the number of open-timer phantom counts is plotted as a function of measured aerodynamic size, the number of open-timer phantom particles increases with aerodynamic diameter. This occurs because the aerodynamic size channels are chosen on a logarithmic scale and the larger particle channels have larger transit time intervals. For instance, with the calibration curve used for this study, the aerodynamic size channel for a 1 μm particle has a width of about 15 ns. At 15 μm, the channel width is about 130 ns.

EXPERIMENTAL PROCEDURES AND RESULTS

The experimental work was done to show that TOF aerosol spectrometers can register open-timer phantom particles and to evalu-

ate whether Eq. 7 adequately describes open-timer phantom particle creation by the mLPP. In addition, experiments were conducted to document the generation of open-timer phantom particles by the SPP. The mLPP, instead of the SPP, was chosen for study for two reasons. First, the pulse detection probability, which is needed to estimate the single pulse concentration and the concentration of open-timer phantom particles, can be estimated from manipulation of the SPP and mLPP accumulator data. For the SPP, the probability of pulse detection and the single pulse concentration are not directly available from the data stored by the APS model 3310. Furthermore, the mLPP's logic prevents it from counting overlap phantom particles, allowing the study of open-timer phantom particles by itself.

Phantom Particle Creation by the Modified Large Particle Processor

The small-scale powder disperser (SSPD, model 3343, TSI, Inc.) was used to aerosolize an aluminum oxide powder (LPA 9, Microabrasives Corp., Westfield, Mass.). This powder had a mass median diameter of 9 μm and 90% of the mass was smaller than 15 μm. The air flow in the SSPD was adjusted to obtain a flow rate of 8 L/min into the 1.9-cm diameter, 200-cm-long horizontal copper pipe shown in Figure 4. At this flow rate, calculations of gravitational settling in laminar flow show that all the particles larger than 11 μm are collected in the settling tube.

The aerosol passed through a cascade impactor (model 266, Sierra Instruments, Carmel Valley, Calif.) at 8 L/min, with a final stage 50% cut diameter at 8.0 μm aerodynamic diameter. As a conservative estimate, all measured particles larger than 10 μm were assumed to be phantom particles. Before passing into the APS, the output of the impactor passed through a 3.9-L cylindrical mixing chamber which damped out concentration fluctuations from the

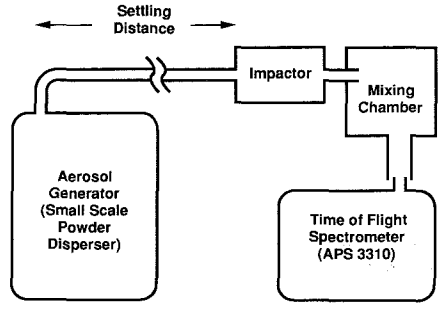

FIGURE 4. Schematic of the equipment for aluminum oxide aerosol measurement, where particles larger than 10 μm are removed before detection by the APS.

SSPD. The concentration in the chamber was varied by adjusting the SSPD's generation rate. Sampling periods of 20 s were used.

Figure 5 displays the number of particles counted by the mLPP as a function of accumulator channel for the aluminum oxide aerosol. Particles larger than 10 μm in Figure 5 should all be open-timer phantom particles. These particles, corresponding to accumulator channels 40–127, are uniformly distributed with respect to transit time (Figure 5). Both KS and chi-squared goodness-of-fit tests did not indicate a significant deviation from a uniform distribution at the 95% confidence level.

The accumulator distributions from the

FIGURE 5. Size dependence of measured aluminum oxide aerosol. The sample time is 300 s. Each accumulator channel is a 66.67-ns increment of transit time.

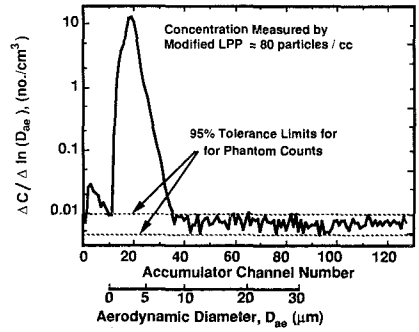

two processors provided the data to calculate the concentration of open-timer phantom counts created by the mLPP. The calculation was based on the count ratio between the mLPP and SPP in the size range where the mLPP was only partially detecting particles. First, however, the SPP open-timer phantom counts were subtracted from the SPP accumulator data. These phantom counts were obtained from part of the SPP distribution, where no real particles were expected to occur (> 10 μm). In addition, the mLPP anticoincidence logic rejected particles over a wider time interval than the SPP. Because the mLPP rejects at least two particles for each coincidence incident, Eq. 1 was used to estimate the fraction of SPP particles that would not be counted if the mLPP were a conventional optical particle counter. Instead of replacing the two overlapping particles with a single larger particle like an optical particle counter, the mLPP deletes both particles from the measured distribution. As a result, coincidence losses by the mLPP estimated from Eq. 1 were multiplied by a factor of 2. The SPP counts were multiplied by this factor to make the counting efficiencies of the SPP and mLPP comparable.

The probability of pulse detection as a function of particle transit time by the mLPP was estimated from the square root of the ratio of the mLPP to the adjusted SPP counts. From the probability of pulse detection, the single pulse concentration in each mLPP channel was computed and these concentrations were summed to compute the single-pulse concentration, $C_{sp,mLPP}$. Then Eq. 7 was used to compute the concentration of open-timer phantom particles larger than 10 μm (accumulator channels 40–127).

Figure 6 presents a comparison of the observed and calculated phantom particle concentrations in channels 40–127. The calculated phantom particle concentration was statistically modeled as a linear function of the observed phantom particle concentration using the form $y = mx + b$. At the 95% confidence level, the slope of the regression line (1.07) did not differ significantly from one and the intercept (0.04) did not differ significantly from zero, indicating agreement between the observed and calculated values.

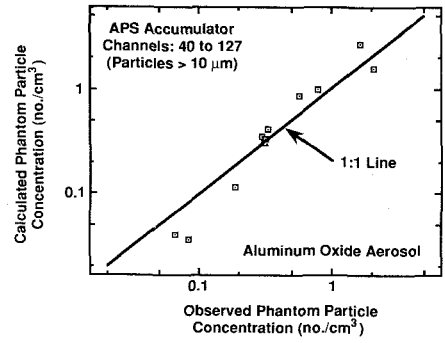

FIGURE 6. Calculated and observed concentration of open-timer phantom particles in the range of channels 40–127. Data and calculations for aluminum oxide aerosol are compared to the line of equality.

Phantom Particle Creation by the Small-Particle Processor

The theoretical section above suggests that open-timer phantom particle creation can be a significant problem with the SPP of the APS. Presently, there is no method to determine *a priori* the concentration of open-timer phantom particles created by the APS's SPP. However, there are a number of experimental techniques which can be used to indicate the extent to which the SPP is creating open-timer phantom particles. To minimize the creation of these phantom particles, one needs to minimize the number of partially detected pulse pairs (resulting in single pulses). For example, this may be accomplished by reducing the pulse amplitude. As particle size decreases, the number of particles often increases. Increasing the size at which particles are detected will, therefore, usually decrease the concentration of single pulses.

To evaluate whether this is a useful ex-

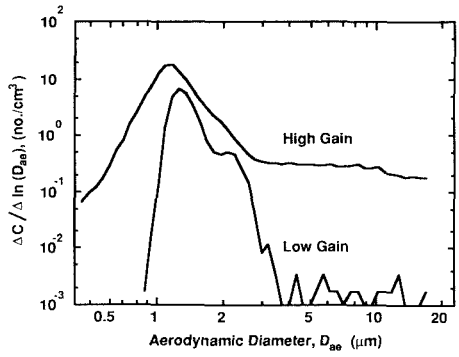

FIGURE 7. Reduction in the concentration of phantom particles produced by reducing photomultiplier gain. Most of the counts above 3 μm are due to open-timer phantom particles.

perimental approach, replicate size distributions were measured with the SPP at high and low gain settings for the photomultiplier tube. The photomultiplier panel readings for these settings were 0.13 and 0.012, respectively. The aerosol was generated by nebulizing a high concentration suspension of 0.8 μm diameter polystyrene latex (PSL) spheres from a nebulizer (Retec Development Co., Portland, Ore.). The distribution was broadened by not drying the aerosol and retaining the agglomerates. After passing through the cascade impactor assembled to remove particles with a 50% cut point of 2.5 μm, the aerosol was sampled by the APS. This aerosol provided a convenient source of partially detected particles which would generate single pulses and phantom particles. The indicated SPP total concentrations were approximately 20 and 1.5 particles/cm^3 at the high and low gain settings, respectively. Figure 7 shows the effect of photomultiplier tube gain upon the apparent aerosol size distribution as measured by the SPP. Decreasing the photomultiplier gain approximately an order of magnitude decreases the true counts about 50% at 1.5 μm and decreases the open-timer phantom counts about two orders of magnitude between 4 and 15 μm. The change in shape of the size distribution between 1.5 and 3 μm is apparently due to incomplete detection of the real particles.

A knowledge of the pulse amplitudes and a comparison of particle size data recorded by the LPP and SPP in their overlap range was used to judge whether phantom particle creation affected SPP results. An aluminum oxide aerosol (LPA 20) was generated using the SSPD. At a flow rate of 5 L/min, the APS sampled this aerosol through the cascade impactor which was assembled to give a 50% cut diameter of 2.5 μm. The LPP was used with the normal 3.0-V threshold. The gain of the photomultiplier tube was adjusted so that particles larger than 8 μm aerodynamic diameter had pulse amplitude greater than 4.0 V. The pulse amplitude was measured with a storage oscilloscope (model 7623 A, with a 7A18 Amplifier, and a 7B85 time base, Tektronix, Inc., Beaverton, Ore.). As recommended in the APS manual, a 50-Ω resistor was placed across the APS analog output. Figure 8 displays the number of counts by the SPP and LPP as a function of particle diameter. There is as much as a 250-fold discrepancy between the number of counts from these two processors in the 5.23–15.39-μm diameter range!

DISCUSSION

Theoretical and Experimental Results

The experimental work supported the results of the theoretical analysis and the Monte Carlo simulations. As theoretically predicted, the mLPP created open-timer phantom particles which were uniformly distributed with respect to transit time (Figure 5). The observed and calculated concentrations of open-timer phantom particles were in agreement (Figure 6). If the single-pulse concentration were directly available from the TOF spectrometer, the user could calculate the concentration of open-timer phantom particles from Equations 5 or 7.

Implications of Findings

The creation of open-timer phantom particles is inherent in the design of TOF aerosol spectrometers. In order to detect a particle

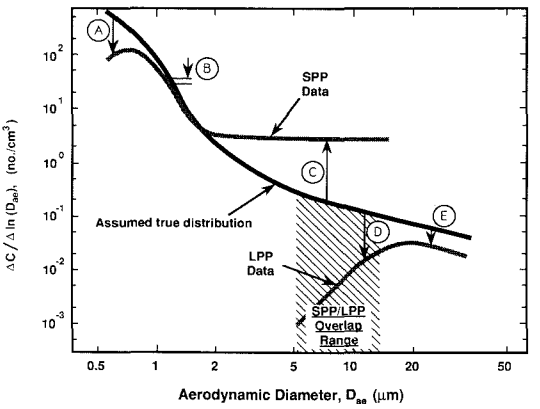

FIGURE 8. Discrepancy between LPP and SPP particle counts. The sampling period was 47 min and the aluminum oxide concentration was 120 particles/cm^3. The annotations illustrate possible sources of error in size distributions measured by the APS 3310. These error sources are: (*A*) SPP detection threshold losses; (*B*) coincidence losses; (*C*) open-timer phantom particle creation; (*D*) LPP detection threshold loss; and (*E*) LPP coincidence losses.

and measure its size, TOF aerosol spectrometers must detect two pulse of light scattered by a particle as it passes through two light beams. For particles whose pulse amplitude is near a detection threshold, the probability of pulse detection is less than 1.0. This inherently leads to the detection of single pulses which can cause the creation of open-timer phantom particles by TOF aerosol spectrometers.

The generation and distribution of open-timer phantom particles will vary with the detection logic of the TOF aerosol spectrometer. For example, the counting rules for the LPP prevent it from counting phantom particles. When the 3-V threshold voltage in the LPP is reduced, this mLPP can also create phantom particles. Furthermore, the Monte Carlo simulations showed that the shape of the open-timer phantom particle distribution created by the SPP differed from the distribution obtained from the mLPP. Thus, the detection logic affects the phantom particle distribution.

The experimental results presented in Figure 8 are annotated to facilitate discussion of the various errors that can occur in TOF spectrometers such as the APS. An assumed true distribution has been drawn into this figure as a reference for the error discussion. Because the presentation is on a log-log scale, some of the errors may be overstated in order to increase the visibility of the annotations. The magnitude of each of the errors is dependent on the concentration and, in some cases, on the size distribution.

Note that, when evaluating particle size distributions obtained from the APS, phantom particle generation primarily affects the tails and minima of the measured distribution. Note also that the APS software normally presents the SPP and LPP results as a single combined distribution, rather than separately as shown in Figure 8.

In the APS, there are different detection thresholds for the SPP and LPP. The SPP threshold produces a lower tail (A) on the measured distribution that typically occurs in the 0.5–1.5-μm size range. The LPP threshold (D) may not be noticed, because of the way the data from the SPP and LPP are combined in the data presentation software. These and other detection thresholds may produce minima in the measured distribution.

The second type of error (B) noted in Figure 8 indicates a loss of particles due to coincidence between two fully detected particles. This occurs for all types of optical particle counters, but is a relatively small fractional change at low particle concentrations. The effect of this coincidence upon the size distribution varies with the TOF spectrometer's data processing system. For example, in the SPP, this type of coincidence causes the two coincident particles to be replaced by smaller, overlap phantom particles (case 3, Figure 1). In the LPP, the

coincident particles are completely eliminated (E) from the measured distribution.

The third type of error (C) in Figure 8 is the open-timer phantom particle count that occurs at all parts of the distribution. However, it only becomes apparent at the tails or minima of the original distribution where there are more phantom counts than real counts. Thus, above about 4 μm in Figure 8, the SPP measured distribution consists almost wholy of open-timer phantom particles. When one uses such data for calculating volume or mass distributions or determining relative concentrations (e.g., penetration measurements), the results will be erroneous.

A more sophisticated logic system built into the detector can eliminate phantom particles. However, such a system can have its own pitfalls, as exemplified by the LPP. The light scattering efficiency of particles varies considerably and it may be necessary to adjust the threshold limits to provide adequate detection of specific types of particles. For instance, the LPP may not detect some of the 5.23–15.39-μm particles, resulting in a notch in the combined SPP/LPP distribution. In addition, the logic used to prevent detection of phantom particles may also prevent the detection of a significant fraction of the real particles.

Several approaches for evaluating the presence of open-timer phantom particles have been indicated. A preselection device, such as a settling chamber or impactor, can be used to remove particles above a certain size. If particles still appear in the measured distribution, they are likely to be the result of coincidence. Open-timer phantom particles are indicated if the size distribution of the measured larger particles changes significantly when the detector gain is reduced as, for example, shown in Figure 8. Similar results have also been reported for the APS model 3300 (Wake, 1989) and in the APS manual (TSI, 1987). This technique of reducing the photomultiplier tube gain to eliminate phantom particles should be used with care, because it may result in incomplete particle detection and a modified size distribution.

Several additional techniques for reducing open-timer phantom particles were considered. These phantom particles were predicted and experimentally found to vary with the square of the concentration of particles near the detection threshold (Figure 6). This suggests dilution of the aerosol as another option for reducing the number of phantom counts. A preselector, such as a virtual impactor, that reduces the concentration of small particles may also have a similar effect. However, such a device adds complexity to the measurement system, as well as the calibration and data analysis.

Alternatively, at low measured concentration when coincidence losses in the LPP are insignificant, the difference between the SPP and the corresponding size LPP counts may be used to determine the average number of phantom particles per channel created by the SPP. In the size range over which the LPP is completely detecting particles, the difference between SPP counts and the corresponding LPP counts is due to open-time phantom particles. This difference can be calculated for several of these channels. However, for this calculation to give a valid estimate of the SPP open-timer phantom counts, the LPP must be fully detecting the particles in the size range over which the differences are being determined. This may not be possible for highly light-absorbing or for high-density particles. Finally, this difference calculation must only be used at very low concentrations or the open-timer phantom counts will be overestimated due to LPP coincidence losses. Equation 1 with $Q = 16.6\ \text{cm}^3/\text{s}$ and $t = 2.52 \cdot 10^{-5}$ s (the LPP's total anticoincidence time period) can be used to estimate the level of LPP coincidence.

After identifying the presence of open-timer phantom particles, it is possible to improve the measured distribution by subtracting the phantom particles from the mea-

sured distribution. For example, by using appropriate aerodynamic preselectors, all of the measured particles larger than a certain size can be assumed to be phantom particles. Then, the expected number of open-timer phantom counts in each channel of particle size data can be estimated.

However, simply subtracting the expected phantom count in each channel from the measured distribution leaves the variability due to the phantom counts in the adjusted distribution. In the size ranges where the phantom particle count exceeds the number of real particles, the number of real particles counted may be less than the statistical fluctuations in the number of phantom counts. The following approach allows the determination of the size range over which the adjusted distribution data is meaningful.

The original number of particles in each size channel "j" has a standard deviation $s_{j,\text{total}}$, based on Poisson statistics. The standard deviation is equal to the square root of the original number of counts in bin j. The phantom count also has a standard deviation $s_{j,\text{phantom}}$ associated with it. Since the adjusted count is equal to the difference between the measured count and the phantom count, the resulting standard deviation, $s_{j,\text{adj.}}$, is computed by pooling $s_{j,\text{phantom}}$ and $s_{j,\text{total}}$. From $s_{j,\text{adj.}}$, one can apply the limits of detection and quantitation used for the reporting of the results of environmental analysis (Keith et al., 1983). At the limit of detection which is $3 \cdot s_{j,\text{adj.}}$, there is a better than 99% probability that the counts in that channel are above the noise. At the limit of quantitation, which is $10 \cdot s_{j,\text{adj.}}$, the uncertainty in the adjusted count is $\pm 30\%$ at the 99% confidence level.

A final technique for evaluating the presence of, and perhaps, correcting for phantom particles is suggested by Eqs. 2–7. If the hardware/software of the TOF aerosol spectrometer records the number of times that the timer has been triggered by a first pulse, but not closed by a second pulse, then this number can be used to calculate the single-pulse concentration. From the single pulse concentration, the concentration of open-timer phantom particles can be computed using Eqs. 2–7. This technique was not tried, since it involved a major modification to the APS.

CONCLUSIONS

As with any instrument, it is important to know the limitations of TOF aerosol spectrometers, which are useful for measuring aerosol size distributions in real time. In these instruments, phantom particles created by the combination of coincidence and the partial detection of aerosol particles can introduce significant errors into the measured size distributions. Phantom particles are spurious particles that are added to the measured size distribution. In creating these phantom particles, real particles are deleted from the measured distribution. The phantom particles are added to all regions of the distribution and can cause relatively large errors in the minima and wings of the distribution. In regions of the size distribution where a relatively large number of real particles are counted, the APS does provide accurate concentration data.

Two data processors in the APS, each optimized for a different part of the size range, can reduce phantom particle production and give a more accurate estimate of the complete size distribution. However, it is important to understand how the processors respond to aerosols with various optical properties in order to fully utilize the additional information and to avoid errors. In addition, integration of the data from the two processors in their overlap range by a simple weighted average may not provide a good estimate of the aerosol distribution.

The number and distribution of open-timer phantom particles can vary with the instrument's detection logic. Several techniques exist for calculating or measuring the concentration of these phantom particles. These techniques have their drawbacks in

terms of speed or accuracy and thus detract from the usefulness of the time-of-flight aerosol spectrometer as a real-time instrument. The manufacturers of these instruments need to avoid this source of error or provide a means of estimating the magnitude of the error. It is suggested that time-of-flight aerosol spectrometers be designed to measure the concentration of single pulses, so that the concentration and distribution of open-timer phantom particles can be estimated and the size distribution data interpreted appropriately.

DISCLAIMER

Mention of company names or products does not constitute endorsement by the National Institute for Occupational Safety and Health.

The support of the U.S. Environmental Protection Agency through interagency agreement DW75931706-01-0 is gratefully acknowledged.

REFERENCES

Baron, P. A. (1986). *Aerosol Sci. Technol.* 5:55-67.

Borland International. (1985). *Turbo Basic Owner's Handbook*. Scotts Valley, Calif.

Dahneke, B. E. (1974). *Aerosol Beam Device and Method*. United States Patent 3,854,321, December 17, 1974.

Gibson, J. D. (1971). *Nonparametric Statistical Inference*. McGraw-Hill, New York, pp. 68-90.

Jaenicke, R. (1972). *J. Aerosol Sci.* 30:95-111.

Julanov, Y., Lushnikov, A., and Nevskii, I. (1984). *J. Aerosol Sci.* 15:69-79.

Keith, L., Crummett, W., Deegan, J., Libby, R., Taylor, J., Wentler, G., and The ACS (American Chemical Society) Committee on Environmental Improvement. (1983). *Anal. Chem.* 55:2210-2218.

Miller, I., and Freund, J. (1977). *Probability and Statistics for Scientists and Engineers*. 2nd edition. Prentice-Hall, Englewood, N. J.

Remiarz, R., Agarwal, J., Quant, F., and Sem, G. (1983). In *Aerosols in the Mining and Industrial Work Environments* (V. Marple and B. Liu, eds.). Ann Arbor Science Publishers, Ann Arbor, Mich., Vol. 3, pp. 879-895.

TSI, Inc. *APS 3300 Manual*. 500 Cardigan Road, St. Paul, Minn.

Wake, D. (1989). *J. Aerosol Sci.* 20:13-17.

Whitney, C. (1984). *Byte*. October, pp. 128-129.

Willeke, K., and Liu, B. Y. H. (1976). In *Fine Particles: Aerosol Generation, Measurement, Sampling, and Analysis*. Academic Press, New York, pp. 698-728.

Received September 21, 1989; accepted July 3, 1990.